Supporting Information

Exceeding three-electron reactions in $Na_{3+2x}Mn_{1+x}Ti_{1-x}(PO_4)_3$ NASICON Cathode with High Energy Density for Sodium-ion Batteries

Jiefei Liu[1], Kangshou Lin[1], Yu Zhao[1], Yu Zhou[1], Xianhua Hou[1,2*], Xiang Liu[1,3], Hongtao Lou[4], Kwok-ho Lam[5], Fuming Chen[1*]

[1] *Guangdong Provincial Key Laboratory of Quantum Engineering and Quantum Materials, Guangdong-Hong Kong Joint Laboratory of Quantum Matter, Guangdong Engineering Technology Research Center of Efficient Green Energy and Environment Protection Materials, School of Physics and Telecommunication Engineering, South China Normal University, Guangzhou 510006, China*

[2] *SCNU Qingyuan Institute of Science and Technology Innovation Co., Ltd., Qingyuan 511517, China*

3 School of Energy Science and Engineering, Institute of Advanced Materials, Nanjing University of Technology, Nanjing 210009, China

[4] *Guangdong Lingguang New Material Co., Ltd, Zhaoqing, 526108, China*

[5] *Department of Electrical Engineering, Hong Kong Polytechnic University, Hunghom, Kowloon, Hong Kong*

E-mail addresses: houxianhua@m.scnu.edu.cn; fmchen@m.scnu.edu.cn

~~Calculation of the theoretical~~ capacity of $Na_{3.4}Mn_{1.2}Ti_{0.8}(PO_4)_3$:

The theoretical capacity is calculated using the formula: C=nF/3.6 M (mAh/g),[1] where n, F, and M represent the transfer electron number per mole material, Faraday constant and molecular weight. Specifically, the theoretical capacity of $NM_{1.2}T_{0.8}P$ can be obtained by the below process: (3.2mol * 96500 C/mol) / (467.3 g/mol * 3.6 C/mAh) = 183.56 mAh g^{-1}.

Calculation of the average voltage: V=E/C, E and C represent energy density and capacity, resppectively. Both data of E and C can read from the Battery LAND CT2001A battery testing system.

Preparation of Full cell and electrochemical test.

The hard carbon (HC) anode was directly purchased from BTR New Energy Materials Inc. The HC anode was cycled for 5 cyles at 100 mA g^{-1} in 1M $NaClO_4$ dissovled EC/DMC with 5%FEC electrolyte. Then the HC anodes were dissambled in a glovebox filled with argon and matched with $NM_{1.2}T_{0.8}P$ cathode 1M $NaClO_4$ dissovled EC/DMC with 5%FEC electrolyte with close to capacity. The $NM_{1.2}T_{0.8}P$ //HC full cell was measured with the voltage window of 0.5-4.2V.

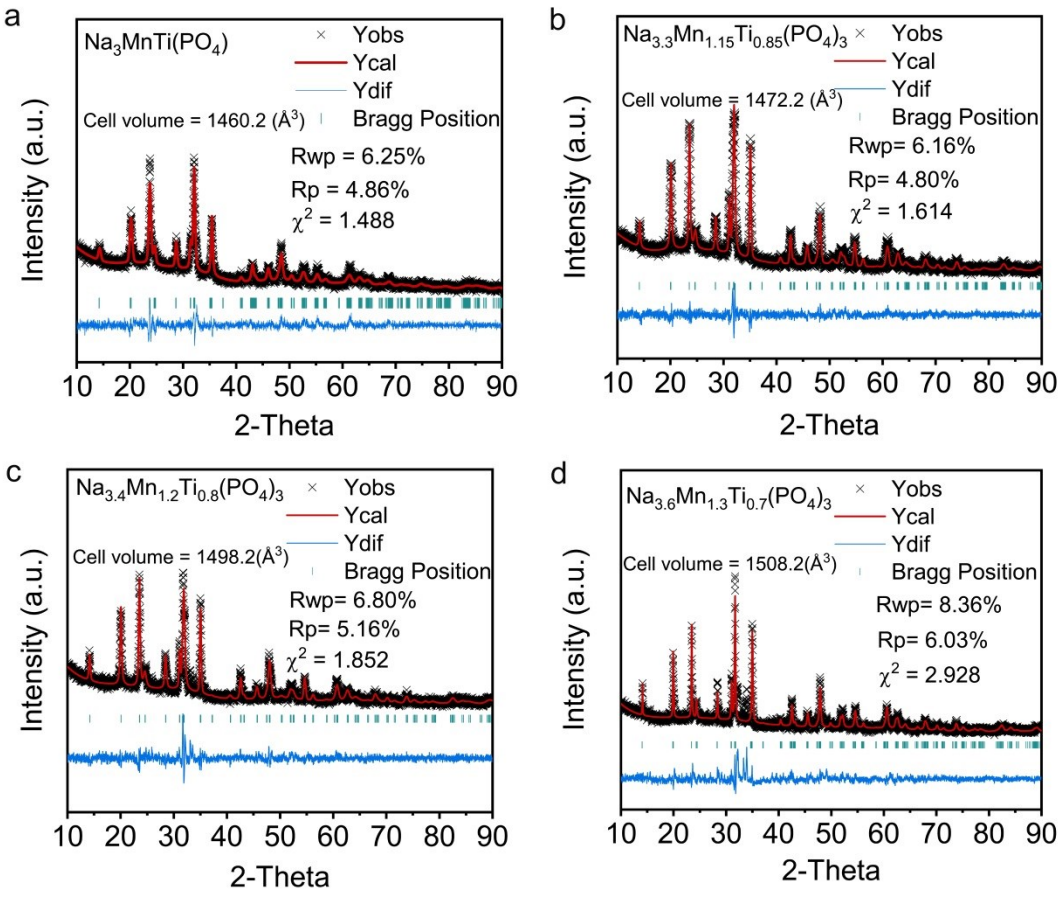

Figure S1. Rietveld refinement of XRD pattern: (a) NMTP. (b) $NM_{1.15}T_{0.85}P$. (c) $NM_{1.2}T_{0.8}P$. (d) $NM_{1.3}T_{0.7}P$.

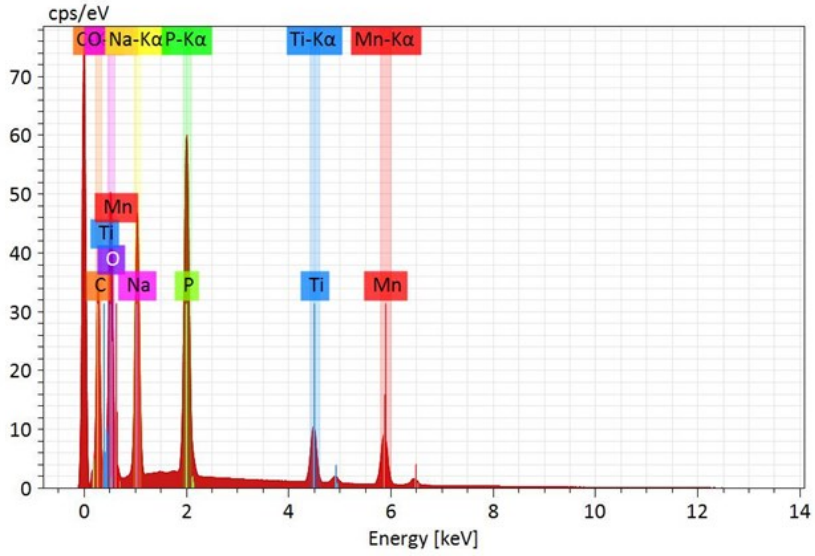

Figure S2. The EDS spectrum of $NM_{1.2}T_{0.8}P$.

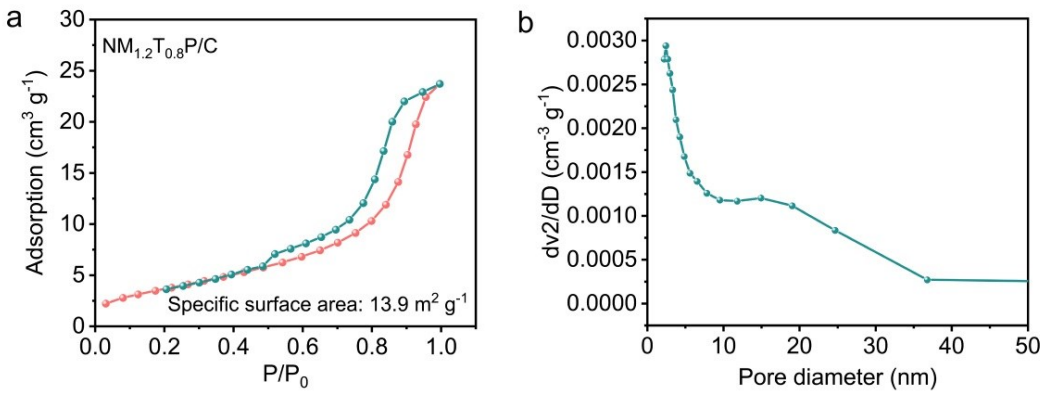

Figure S3. (a) The N_2 absorption-desorption isotherms of $NM_{1.2}T_{0.8}P$. (b) The corresponding pore dize distribution curves.

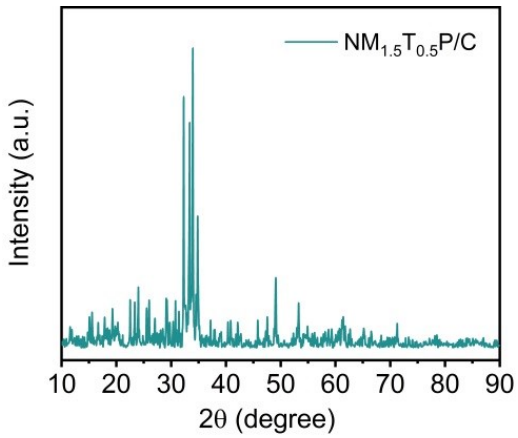

Figure S4. The XRD pattern of $NM_{1.5}T_{0.5}P$ sample.

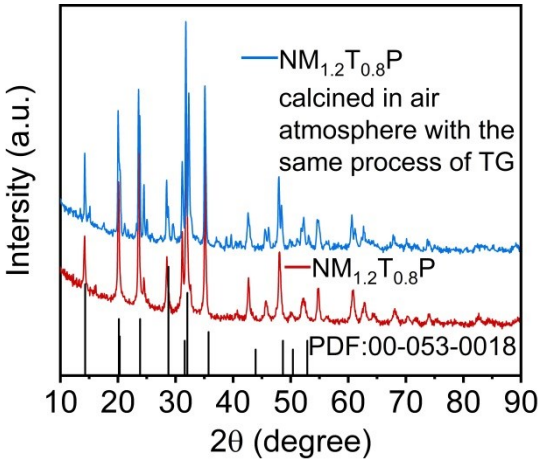

Figure S5. The XRD patterns of $NM_{1.2}T_{0.8}P$ and $NM_{1.2}T_{0.8}P$ calcined in air with the same heating process of TG.

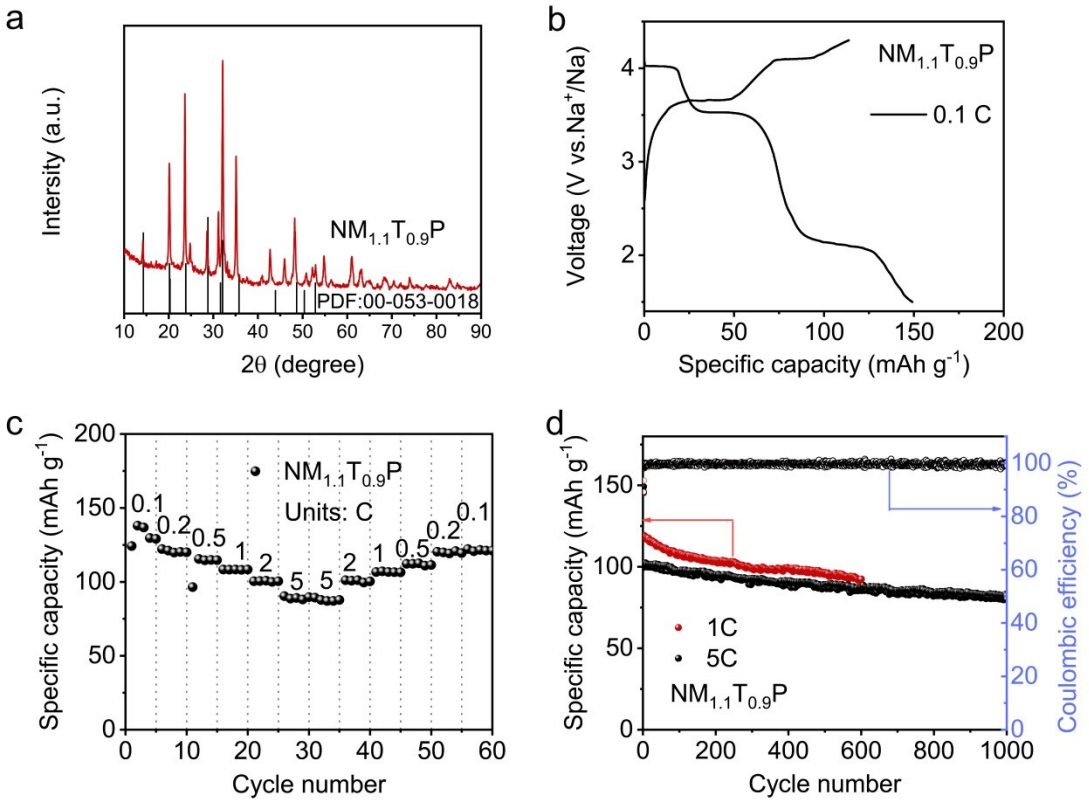

Figure S6. (a) The XRD pattern of $NM_{1.1}T_{0.9}P$. (b) The charge/discharge profile of $NM_{1.1}T_{0.9}P$ at 0.1C. (c) The rate performance of $NM_{1.1}T_{0.9}P$. (d) The long cycling performance of $NM_{1.1}T_{0.9}P$ at 1C and 5C.

The prepared $NM_{1.1}T_{0.9}P$ sample possesses a typical NASICON structure, which can deliver a highest capacity of 149.1 mAh g^{-1} at 0.1C. The $NM_{1.1}T_{0.9}P$ exhibits a superior cycling stability, which can deliver a reversible capacity of 119 mAh g^{-1} at 1C and retain 81% capacity retention after 500 cycles. Even at large current of 5C, the $NM_{1.1}T_{0.9}P$ can still deliver a reversible capacity of 100.2 mAh g^{-1} with the 81.5% capacity retention after 1000 cycles.

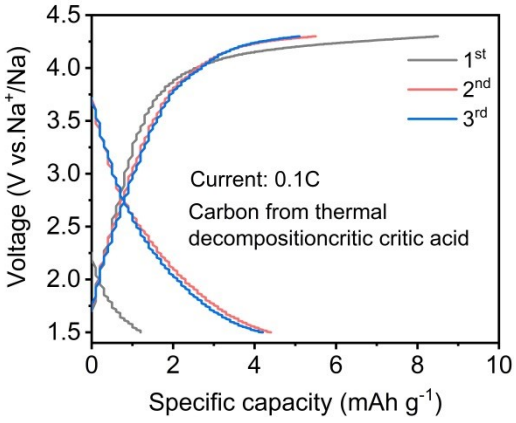

Figure S7. The charge/discharge profiles of carbon derived from critic acid at 15mA g^{-1} within the voltage window of 1.5-4.3V.

Within the voltage window of 1.5 to 4.3V, the carbon derived from critic acid can only deliver a reversible capacity of 4 mAh g^{-1} at 0.1C (Fig. S7). Therefore, the capacity contribution of carbon in $NM_{1.2}T_{0.8}P$ compounds can be negligible.

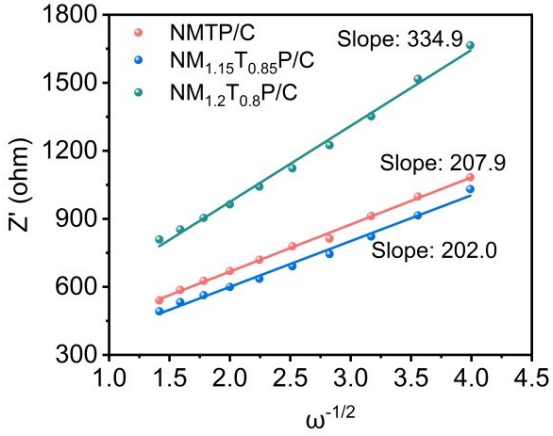

Figure S8. The linear relationships between Z' and reciprocal square root of angular rate ($\omega^{-1/2}$) in the low-frequency region.

For EIS, the diffusion coefficient of Na^+ can be calculated with this equation: $D_{Na+} = R^2T^2/2A^2n^2F^4C^2\sigma^2$. Where R is gas constant, T is the absolute temperature, F is Faraday constant, A is surficial area of the electrode, n is the number of transferred electrons, C is the concentration of Na^+ in the lattice, and σ is the Warburg factor and can be obtained from the line of $Z' \sim \omega$-1/2. Because the $NM_{1.15}T_{0.85}P$ possesses the smallest σ value and the σ value of $NM_{1.2}T_{0.8}P$ is largest, D_{Na+} of $NM_{1.15}T_{0.85}P$ is largest and D_{Na+} of $NM_{1.2}T_{0.8}P$ is smallest.

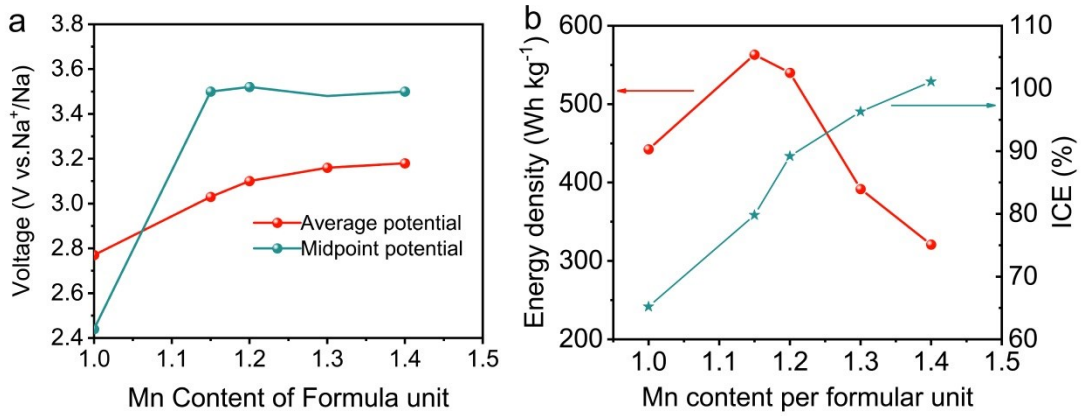

Figure S9. (a) The midpoint potential and average potential of $N_{3+2x}M_{1+x}T_{1-x}P$ at 0.1 C. (b) The corresponding energy density and initial coulombic efficiency.

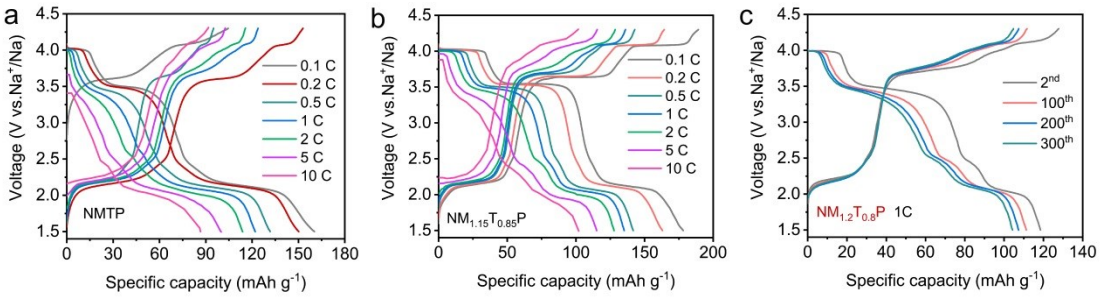

Figure S10. (a) The rate charge/discharge curves of NMTP. (b) The rate charge/discharge curves of $NM_{1.15}T_{0.85}P$. (c) The charge/discharge curves of $NM_{1.2}T_{0.8}P$ at 1 C after 100, 200, and 300 cycles.

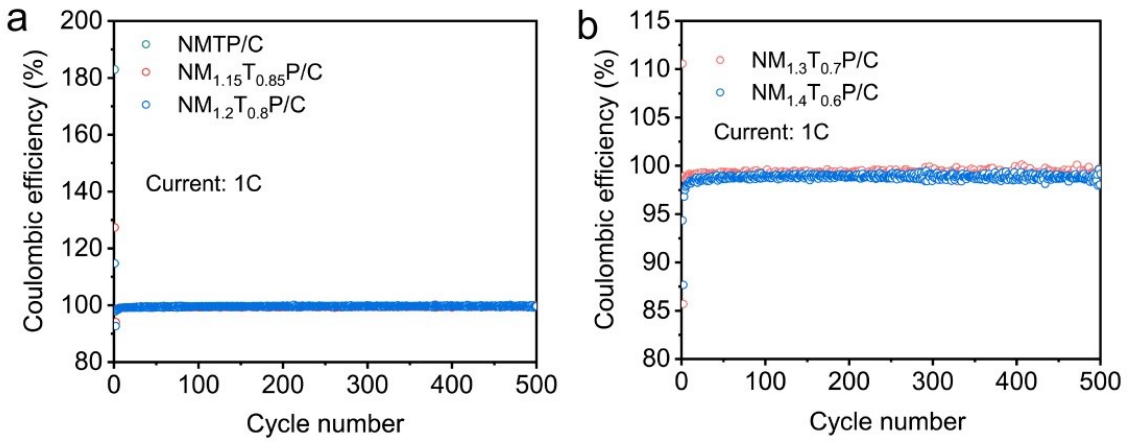

Figure S11. (a) The corresponding coulombic efficiency of NMTP, $NM_{1.15}T_{0.85}P$, and $NM_{1.2}T_{0.8}P$ at 1 C. (b) The corresponding coulombic efficiency of $NM_{1.3}T_{0.7}P$, and $NM_{1.4}T_{0.6}P$ at 1 C.

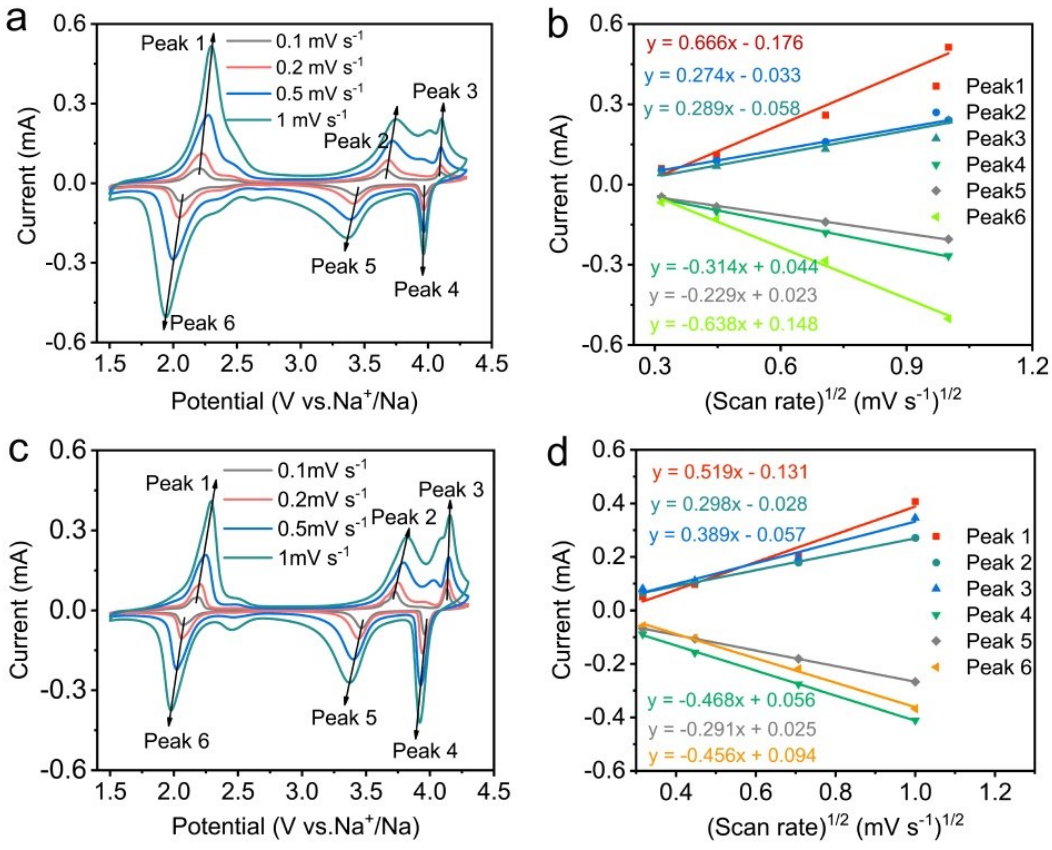

Figure S12. (a) CV curves of NMTP cathode under different scan rates. (b) The corresponding linear relationships between I_p and $v^{1/2}$ of different redox peaks. (c) CV curves of $NM_{1.15}T_{0.85}P$ cathode under different scan rates. (d) The corresponding linear relationships between I_p and $v^{1/2}$ of different redox peaks.

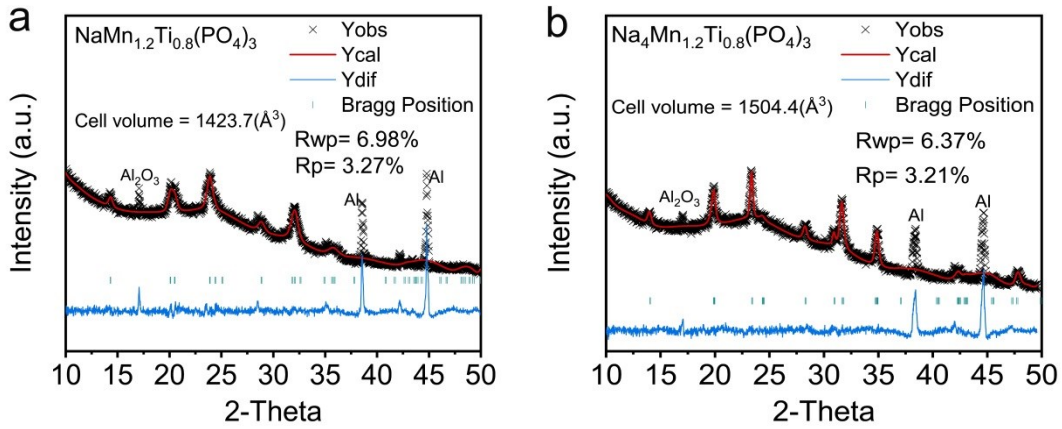

Figure S13. (a) The Rietveld refinement for XRD pattern of $NM_{1.2}T_{0.8}P$ charged to 4.3V. (b) The Rietveld refinement for XRD pattern of $NM_{1.2}T_{0.8}P$ discharged to 1.5V.

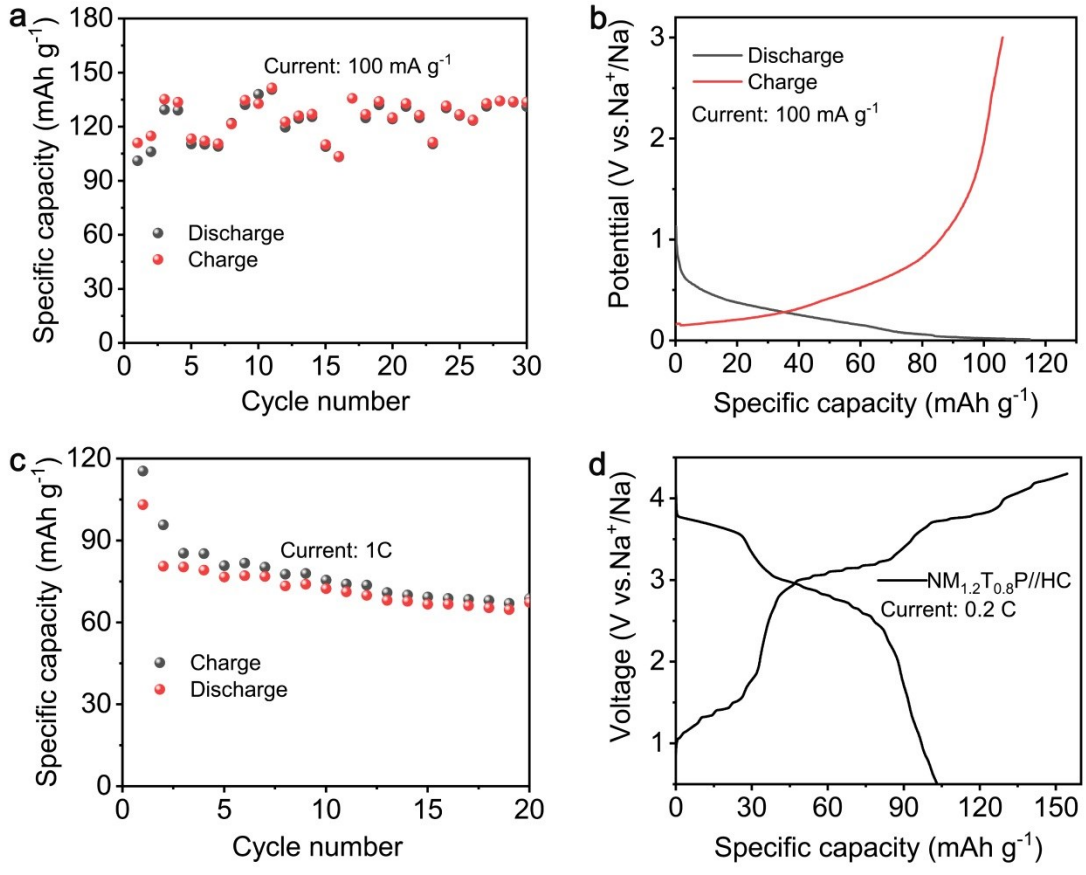

Figure S14. (a) The cycling performance of hard carbon anode at 100 mA g^{-1}. (b) The charge/discharge profiles of hard carbon anode at 100 mA g^{-1}. (c) The cycling performance of $NM_{1.2}T_{0.8}P$//HC full cell at 1C (150 mA g^{-1}). (d) The charge/discharge profiles of $NM_{1.2}T_{0.8}P$//HC full cell at 0.2C.

After fully charged state, the full cell exhibits a potential of 3.77V. At 0.2C, the full cell can deliver a specific capacity of 103.2 mAh g^{-1}. After 20 cycles at 1C, the full cells can retain capacity retention of 76.1%. The hard carbon anode was directly purchased from BTR New Energy Materials Inc. Therefore, the anodes don't exhibit superior property which may cause the poor performance of full cell.

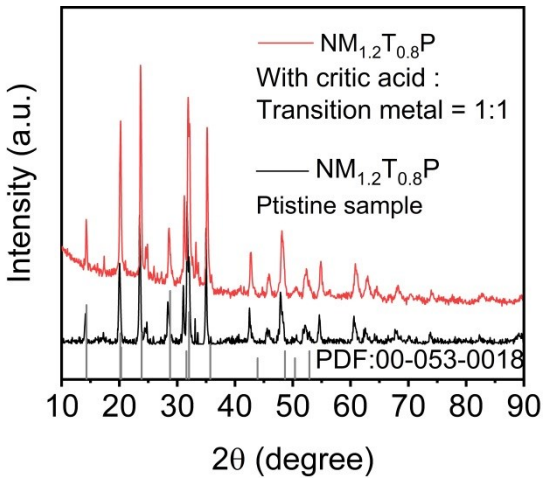

Fig. S15. The XRD pattern of $NM_{1.2}T_{0.8}P$ with decreasing critic acid content during synthesis process.

Table S1. ICP-OES chemical analysis results of $NM_{1.2}T_{0.8}P$

Elements	Na	Mn	Ti
W/W%	13.4387	12.1339	6.739457
Atomic ratio	4.17	1.57	1

Table S2. The fitted value of Rct from EIS

Samples	NMTP/C	$NM_{1.15}T_{0.85}P$/C	$NM_{1.2}T_{0.8}P$/C
Rct/Ω	271.7	342.4	452.3

Table S3. The evaluated D_{Na+} from CV curves.

Sample	Peak1	Peak2	Peak3	Peak4	Peak5	Peak6
NMTP/ $cm^2\ s^{-1}$	4.27×10^{-10}	7.23×10^{-11}	8.0×10^{-11}	9.5×10^{-11}	5.05×10^{-11}	3.92×10^{-11}
$NM_{1.15}T_{0.85}P$/ $cm^2\ s^{-1}$	2.59×10^{-10}	8.55×10^{-11}	1.46×10^{-10}	2.11×10^{-10}	8.16×10^{-11}	2.0×10^{-10}
$NM_{1.2}T_{0.8}P$/ $cm^2\ s^{-1}$	5.83×10^{-11}	6.02×10^{-11}	1.07×10^{-10}	8.32×10^{-11}	5.1×10^{-11}	5.23×10^{-11}

Table S4. The fitted lattice parameters of various samples based on Rietveld refinement.

Sample	a/ Å	c/ Å	Volume/ $Å^3$
NMTP	8.80	21.76	1460.2
$NM_{1.15}T_{0.85}P$	8.86	21.64	1472.2
$NM_{1.2}T_{0.8}P$	8.90	21.83	1498.2
$NM_{1.3}T_{0.7}P$	8.90	21.98	1508.2

Table S5. The energy density comparison with reported various cathode materials for SIBs.

Sample	Current density mA/g	Specific capacity mAh/g	Energy density Wh/kg	Reference
$NM_{1.15}T_{0.85}P$	15	181.4	560.2	This work
$NM_{1.2}T_{0.8}P$	15	176.1	539.5	This work
$Na_3MnTi(PO_4)_3$	15	160.3	442	This work
$Na_4MnCr(PO_4)_3$	5.5	131	470	Ref [2]
$Na_4Fe_3(PO_4)_2(P_2O_7)$	12.9	128	357.5	Ref [3]
$Na_3MnTi(PO_4)_3$	23.4	114	410	Ref [4]
$Na_3V_2(PO_4)_3$	58.8	116.3	382.9	Ref [5]
$Na_4MnCr(PO_4)_3$	16	160.5	566.5	Ref [6]
$Na_3V_2(PO_4)_2F_3$	128	119.9	446.4	Ref [7]
$Na_4MnV(PO_4)_3$	55	109.8	380	Ref [8]
$Na_{3.5}Mn_{0.5}V_{1.5}(PO_4)_3$	110	109.1	373.5	Ref [9]
$Na_4Mn_2Co(PO_4)_2P_2O_7$	12.9	96.1	371	Ref [10]
$Na_{3.1}Fe_4[Fe(CN)_6]_3$	12	123	344	Ref [11]
$Na_{0.78}Ni_{0.23}Mn_{0.69}O_2$	12.1	138	448.5	Ref [12]
$Na_{0.75}Ni_{0.82}Co_{0.12}Mn_{0.06}O_2$	20	171	478.8	Ref [13]
$Na_3V_{2-x}Fe_x(PO_4)_2F_3$	12.8	118	433	Ref [14]

Table S6. Detailed structural information of NMTP derived from Rietveld refinement

space group = R-3c	R_p = 4.86%		R_{wp} = 6.25%			
a (Å) = 8.801568	c (Å) = 21.765656		α (°) = 90			
β (°) = 90	γ (°) = 120		V ($Å^3$) = 1460.234			
Atom	x	y	z	Mult	Occupancy	Uiso
Na1	0.000000	0.000000	0.000000	6	0.8830	0.165000
Na2	0.639149	0.000000	0.250000	18	0.6984	0.007700
Mn	0.000000	0.000000	0.149350	12	0.5000	0.040591
Ti	0.000000	0.000000	0.149350	12	0.5000	0.071422
P	0.298300	0.000000	0.250000	18	1.0000	0.031300
O1	0.186680	0.176844	0.079159	36	1.0000	0.008812
O2	0.026290	0.205683	0.195142	36	1.0000	0.035081

Table S7. Detailed structural information of $NM_{1.15}T_{0.85}P$ derived from Rietveld refinement

space group = R-3c	R_p = 4.80%		R_{wp} = 6.16%			
a (Å) = 8.863012	c (Å) = 21.641275		α (°) = 90			
β (°) = 90	γ (°) = 120		V ($Å^3$) = 1472.283			
Atom	x	y	z	Mult	Occupancy	Uiso
Na1	0.000000	0.000000	0.000000	6	0.8909	0.019783
Na2	0.642032	0.000000	0.250000	18	0.7838	0.039920
Mn	0.000000	0.000000	0.149406	12	0.5750	0.022073
Ti	0.000000	0.000000	0.149406	12	0.4250	0.053507
P	0.298300	0.000000	0.250000	18	1.000	0.022137
O1	0.186680	0.176844	0.079159	36	1.000	0.08238
O2	0.026290	0.205683	0.195142	36	1.000	0.00676

Table S8. Detailed structural information of $NM_{1.2}T_{0.8}P$ derived from Rietveld refinement

space group = R-3c	R_p = 5.16%		R_{wp} = 6.80%			
a (Å) = 8.902052	c (Å) = 21.831387		α (°) = 90			
β (°) = 90	γ (°) = 120		V ($Å^3$) = 1498.208			
Atom	x	y	z	Mult	Occupancy	Uiso
Na1	0.000000	0.000000	0.000000	6	0.9120	0.00622
Na2	0.642032	0.000000	0.250000	18	0.7053	0.02630
Mn	0.000000	0.000000	0.148938	12	0.6000	0.06436
Ti	0.000000	0.000000	0.148938	12	0.4000	0.00054
P	0.298300	0.000000	0.250000	18	1.000	0.03838
O1	0.186680	0.176844	0.079159	36	1.000	0.02210
O2	0.026290	0.205683	0.195142	36	1.000	0.06329

Table S9. Detailed structural information of $NM_{1.3}T_{0.7}P$ derived from Rietveld refinement

space group = R-3c	R_p = 6.03%		R_{wp} = 8.36%			
a (Å) = 8.900	c (Å) = 21.982		α (°) = 90			
β (°) = 90	γ (°) = 120		V ($Å^3$) = 1508.200			
Atom	x	y	z	Mult	Occupancy	Uiso
Na1	0.000000	0.000000	0.000000	6	0.9432	0.00622
Na2	0.642032	0.000000	0.250000	18	0.8800	0.02630
Mn	0.000000	0.000000	0.149350	12	0.650	0.01125
Ti	0.000000	0.000000	0.149350	12	0.350	0.00896
P	0.298300	0.000000	0.250000	18	1.000	0.03130
O1	0.186680	0.176844	0.079159	36	1.000	0.03290
O2	0.026290	0.205683	0.195142	36	1.000	0.02600

Table S10. The sodium storage performance comparison with reported NMTP.

Sample	Specific Capacity/ mAh g^{-1}	ICE	Reaction electron number	Energy density Wh kg^{-1}	Reference
NMTP/C	80	70%	2	-	Ref [15]
NMTP/C@rGO	114	-	2	410	Ref [4]
NMTP/C	173	-	3	-	Ref [1]
rGO@NMTP-C	173	-	3	Over 500	Ref [16]
$NM_{1.2}T_{0.8}$	176	91.8	3.07	539	This work
$NM_{1.15}T_{0.85}P$	181.4	80.3	3.13	560	This work

Table S11. The lattice parameters comparison with reported NMTP.

Material	a (Å)	c (Å)	V ($Å^3$)	Reference
NMTP	8.801568	21.765656	1460.234	This work
NMTP	8.82621	21.72350	1465.578	Ref [16]
NMTP	8.8343	21.6654	1464.35	Ref [1]

References:

1. T. Zhu, P. Hu, X. Wang, Z. Liu, W. Luo, K. A. Owusu, W. Cao, C. Shi, J. Li, L. Zhou and L. Mai, *Adv. Energy Mater.* , 2019, **9**, 1803436.
2. J. Wang, Y. Wang, D. H. Seo, T. Shi, S. Chen, Y. Tian, H. Kim and G. Ceder, *Adv. Energy Mater.* , 2020, **10**, 1903968.
3. T. Yuan, Y. Wang, J. Zhang, X. Pu, X. Ai, Z. Chen, H. Yang and Y. Cao, *Nano Energy*, 2019, **56**, 160-168.
4. T. Zhu, P. Hu, C. Cai, Z. Liu, G. Hu, Q. Kuang, L. Mai and L. Zhou, *Nano Energy*, 2020, **70**, 104548.
5. X. Cao, A. Pan, B. Yin, G. Fang, Y. Wang, X. Kong, T. Zhu, J. Zhou, G. Cao and S. Liang, *Nano Energy*, 2019, **60**, 312-323.
6. J. Zhang, Y. Liu, X. Zhao, L. He, H. Liu, Y. Song, S. Sun, Q. Li, X. Xing and J. Chen, *Adv. Mater.*, 2020, **32**, 1906348.
7. L. Deng, F.-D. Yu, Y. Xia, Y.-S. Jiang, X.-L. Sui, L. Zhao, X.-H. Meng, L.-F. Que and Z.-B. Wang, *Nano Energy*, 2021, **82**, 105659.
8. H. Li, T. Jin, X. Chen, Y. Lai, Z. Zhang, W. Bao and L. Jiao, *Adv. Energy Mater.* , 2018, **8**, 1801418.
9. J. Zhang, X. Zhao, Y. Song, Q. Li, Y. Liu, J. Chen and X. Xing, *Energy Storage Materials*, 2019, **23**, 25-34.
10. L. Tang, X. Liu, Z. Li, X. Pu, J. Zhang, Q. Xu, H. Liu, Y. G. Wang and Y. Xia, *ACS Appl. Mater. Interfaces*, 2019, **11**, 27813-27822.
11. W. Ren, Z. Zhu, M. Qin, S. Chen, X. Yao, Q. Li, X. Xu, Q. Wei, L. Mai and C. Zhao, *Adv. Funct. Mater.*, 2019, **29**.
12. C. Ma, J. Alvarado, J. Xu, R. J. Clement, M. Kodur, W. Tong, C. P. Grey and Y. S. Meng, *J. Am. Chem. Soc.*, 2017, **139**, 4835-4845.
13. J. Yang, M. Tang, H. Liu, X. Chen, Z. Xu, J. Huang, Q. Su and Y. Xia, *Small*, 2019, **15**, e1905311.
14. J. Y. Park, Y. Shim, Y.-i. Kim, Y. Choi, H. J. Lee, J. Park, J. E. Wang, Y. Lee, J. H. Chang, K. Yim, C. W. Ahn, C.-W. Lee, D. K. Kim and J. M. Yuk, *J. Mater. Chem. A,*, 2020, **8**, 20436-20445.
15. H. Gao, Y. Li, K. Park and J. B. Goodenough, *Chem. Mater.* , 2016, **28**, 6553-6559.
16. H. Li, M. Xu, C. Gao, W. Zhang, Z. Zhang, Y. Lai and L. Jiao, *Energy Storage Materials*, 2020, **26**, 325-333.